Ionics (2015) 21:2091–2100
DOI 10.1007/s11581-015-1469-0

SHORT COMMUNICATION

Li_2ZrO_3-coated $LiNi_{0.6}Co_{0.2}Mn_{0.2}O_2$ for high-performance cathode material in lithium-ion battery

Shuting Sun[1] · **Chenqiang Du**[2] · **Deyang Qu**[3] · **Xinhe Zhang**[3] · **Zhiyuan Tang**[2]

Received: 14 January 2015 / Revised: 22 April 2015 / Accepted: 17 May 2015 / Published online: 6 June 2015

Abstract To improve the high-rate capacity and cycle ability, Li_2ZrO_3 was successfully coated on $LiNi_{0.6}Co_{0.2}Mn_{0.2}O_2$ materials via wet chemical method. The crystal structure and electrochemical properties of the bare and coated material are studied by X-ray diffractometry (XRD), scanning electron microscope (SEM), transmission electron microscopy (TEM), cyclic voltammetry, and electrochemical impedance spectroscopy (EIS). The XRD and SEM results indicated that the lattice structure of Li_2ZrO_3-coated materials was the same as the pristine one. Transmission electron microscopy showed that there was a thin Li_2ZrO_3 coating layer on the surface. Li_2ZrO_3-coating improves the rate performance and cycling stability. Within the cutoff voltage of 2.6–4.8 V, the 1 wt% Li_2ZrO_3-coated samples exhibited an initial discharge capacity of 190 mAh g^{-1} and with a capacity retention about 85 % after 50 cycles at 0.1 C. Minor Li_2ZrO_3 modification plays an important role to enhance the high-rate capability and cycle ability of $LiNi_{0.6}Co_{0.2}Mn_{0.2}O_2$.

Keywords Li-ion batteries · Cathodes · Charging/discharging · Electrodes · Lithium batteries

✉ Shuting Sun
782473584@qq.com

[1] Department of Chemical Engineering, School of Chemical Engineering and Technology, Tianjin University, Tianjin 300072, China

[2] Department of Applied Chemistry, School of Chemical Engineering and Technology, Tianjin University, Tianjin 300072, China

[3] McNair Technology Company, Limited, Dongguan City, Guangdong 523700, China

Introduction

Lithium-ion batteries have the highest energy density among all available rechargeable batteries, and they have been widely used in portable electric devices. Research on the electrode materials which act as the most important part of batteries has been investigated greatly [1–6]. $LiCoO_2$ was one of the earliest cathode materials generally used, and it remains a primary component for cathodes in rechargeable lithium-ion batteries because of its high voltage and good cycle properties. However, the relatively high cost and toxicity of cobalt, the poor thermal stability of charged Li_xCoO_2 and the lure of larger specific capacity have led to the study of other possible cathode materials for lithium-ion batteries. Recently, a series of layer-structured $Li(Ni_{1-x-y}Co_xMn_y)O_2$ have attracted a great deal of interest because it combines higher specific capacity, lower cost, and considerable cycling performance. Among them, $LiNi_{0.6}Co_{0.2}Mn_{0.2}O_2$ electrode material as one of the most attractive cathode materials has been studied extensively due to its enhanced safety, reduced cost, and increased energy density [7–10]. However, there are still several drawbacks limiting its application in high power lithium-ion batteries for EV and HEV such as its poor rate capability due to its lower electronic conductivity compared to $LiCoO_2$ [11–13] and thermal stability.

In order to further improve the electrochemical properties, many strategies were proposed such as metal doping and surface coating. However, doping with electrochemically inactive elements could stabilize the structure but causes a decrease in capacity because the substituents are usually electrochemically inactive ingredients, such as Al, Mg, and Zn [14–16]. Surface coating of the cathode material by coating a small amount of inert metal oxides, such as ZnO [17], ZrO_2 [18], La_2O_3 [19], and V_2O_5 [20], can significantly improve the cyclic performance by avoiding the unwanted reactions on the

surface. However, the inert metal oxides are often poor electronic and ionic conductors, which usually leads to a large irreversible capacity and poor rate performance. Recently, some Li-contained oxides, such as Li_2CO_3, $LiAlO_2$, $LiCoO_2$, and $Li_4Ti_5O_{12}$ [21–24], were introduced as coating materials for $Li(Ni_{1-x-y}Co_xMn_y)O_2$ electrode, since it availably enhance the electrochemical performance because of their good conductivity and also provide the tunnel for Li^+ transportation during charge/discharge process [18, 25–27].

In this work, Li_2ZrO_3 was introduced as a coating material for $LiNi_{0.6}Co_{0.2}Mn_{0.2}O_2$ cathode. The coated sample was prepared via a wet chemical method followed by heat treatment. X-ray diffractometry, scanning, and transmission electron microscopy have been conducted to confirm the structure and surface morphology. The effect of Li_2ZrO_3 coating on the electrochemical performance and cyclic stability was investigated at a high cutoff voltage, and the reason of the improved performance was discussed.

Experimental

Synthesis of $LiNi_{0.6}Co_{0.2}Mn_{0.2}O_2$ and Li_2ZrO_3-coated cathode materials

The sample of $LiNi_{0.6}Co_{0.2}Mn_{0.2}O_2$ (LNCMO) was prepared by sol–gel method using glycine as the cheating reagent. Stoichiometric amounts of $Ni(CH_3COO)_2{\cdot}4H_2O$, $Co(CH_3COO)_2{\cdot}4H_2O$, $Mn(CH_3COO)_2{\cdot}4H_2O$, and $LiCH_3COO{\cdot}2H_2O$ (5 % excess to compensate for the lithium evaporation during high-temperature calcination) were dissolved in a certain amount of deionized water. The dissolved solution was dropped to a continuously stirred water solution of glycine. After adjusting the pH value to 7–8 with ammonium hydroxide, the solution was stirred at 50 °C for 4 h to ensure the fully mixing. The mixing solution was evaporated at 80 °C until a gel was obtained. The prepared gel was dried at 120 °C in the vacuum drying oven for 12 h and then preheated at 450 °C for 5 h in air. The precursor was grinded and then annealed in air at 900 °C for 20 h with a heating rate of 3 °C min^{-1} to obtain the final power. The powder was grinded and marked as LNCM.

To coat the $LiNi_{0.6}Co_{0.2}Mn_{0.2}O_2$ material with Li_2ZrO_3, stoichiometric amounts of $Zr(NO_3)_4{\cdot}5H_2O$ and $LiCH_3COO{\cdot}2H_2O$ were dissolved in a certain amount of ethanol under stirring at room temperature by a magnetic stirrer until a clear solution was obtained. And then, the prepared $LiNi_{0.6}Co_{0.2}Mn_{0.2}O_2$ powers were dispersed into the solution with constant stirrer and evaporated at 80 °C until the ethanol was evaporated sufficiently. The mixture was heated at 500 °C for 5 h in air to obtain the Li_2ZrO_3-coated $LiNi_{0.6}Co_{0.2}Mn_{0.2}O_2$. The expected amounts of Li_2ZrO_3 were about 1, 3, 5 wt% of the $LiNi_{0.6}Co_{0.2}Mn_{0.2}O_2$ powers, and the coated samples were marked as 0.01 LZO-LNCMO, 0.03 LZO-LNCMO, 0.05 LZO-LNCMO, respectively.

Characterization of the pristine and Li_2ZrO_3-coated $LiNi_{0.6}Co_{0.2}Mn_{0.2}O_2$

Power X-ray diffraction (Rint-2000, Rigaku, Japan) measurements using Cu Kα radiation were used to characterize the structure of the powers. The X-ray diffraction patterns were collected at a scan rate of 3° min^{-1} from 5 to 75°. The particle shape and morphology images of $LiNi_{0.6}Co_{0.2}Mn_{0.2}O_2$ were obtained with a scanning electron microscope (SEM, Hitachi S-3500N). The surface morphologies of the coated samples were analyzed using a transmission electron microscope (TEM, JEOL-JEM 2100F) operated at 200 kV.

Electrochemical measurements

The electrochemical performances of the samples were obtained by using a coin-type cell (CR2032). Cells were consisted of the positive electrode and the lithium-metal negative electrode separated by a porous polypropylene film. The positive electrodes were fabricated from a 80:10:10 (wt.%) mixture of the prepared power/Super P/polyvinylidenefluoride (PVDF). The mixture was dissolved in N-methylpyrrolidinone (NMP) homogeneously under stirring. The slurry was casted on a thin aluminum foil by using a doctor blade, then dried at 120 °C for 12 h in a vacuum oven. The material loading of the cathode electrode is 2.5–2.7 mg cm^{-2}. Lithium coin cell was assembled in a glove box by using the electrolyte 1 M $LiPF_6$ dissolved in ethylene carbonate, dimethyl carbonate, and ethylmethyl carbonate with a 1:1:1 volume ratio and a separator (Celgard 2300). The O_2 and H_2O contents for the glove box were maintained below 2 ppm.

The galvanostatic charge and discharge tests were carried out at room temperature on battery test system (Land CT 2001A, Wuhan, China) at various C rates within the cutoff voltage of 2.6–4.8 V. Impedance measurements of the pristine and the Li_2ZrO_3-coated samples after 10th cycle were conducted on the electrochemical workstation (Gamry PC14–750) in the frequency range of 100 kHz to 0.01 Hz using a voltage vibration of 5 mV. The EIS results were simulated using ZVIEW software. Cyclic voltammetry measurements were recorded between 2.6 and 4.8 V at a sweep rate of 0.1 mV s^{-1} in lithium cells on an electrochemical workstation (CHI1040B, ChenHua, China) at ambient temperature.

Results and discussion

The crystal structure of the bare and Li_2ZrO_3-coated $LiNi_{0.6}Co_{0.2}Mn_{0.2}O_2$ materials with different weight amounts of Li_2ZrO_3 was investigated in Fig. 1. The powers were well-

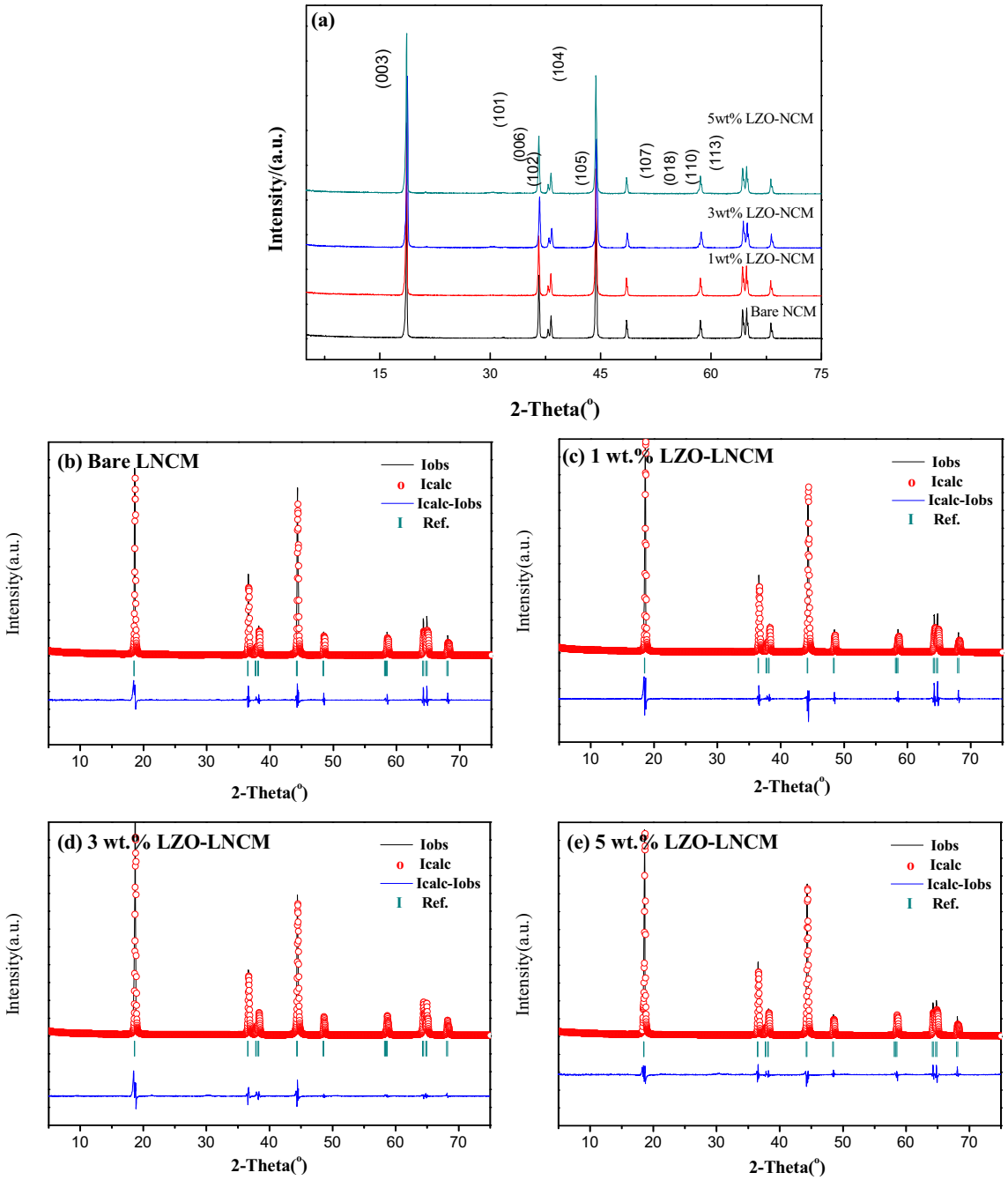

Fig. 1 X-ray diffraction patterns (**a**) and Rietveld refinement results (**b**, **c**, **d**, **e**) of bare and Li_2ZrO_3 (LZO)-coated $LiNi_{0.6}Co_{0.2}Mn_{0.2}O_2$ (LNCMO)

defined hexagonal α-$NaFeO_2$ structure with a space group of R-3m. No impurity peaks corresponding to Li_2ZrO_3-coated materials were observed from the XRD patterns shown in Fig. 1. The structural analyses were conducted on the recorded

Table 1 Lattice parameters from the Rietveld refinement of $LiNi_{0.6}Co_{0.2}Mn_{0.2}O_2$ (LNCMO) and Li_2ZrO_3-coated $LiNi_{0.6}Co_{0.2}Mn_{0.2}O_2$

Sample	Lattice parameter a (Å)	Lattice parameter c (Å)	Lattice parameter (c/a)	Intensity ratio $I_{(003)}/I_{(104)}$
Pure-LNCMO	2.871466	14.220705	4.952420	1.26
1 wt% LZO-LNCMO	2.871993	14.222669	4.952195	1.45
3 wt% LZO-LNCMO	2.872098	14.228609	4.954082	1.36
5 wt% LZO-LNCMO	2.873259	14.231836	4.953203	1.35

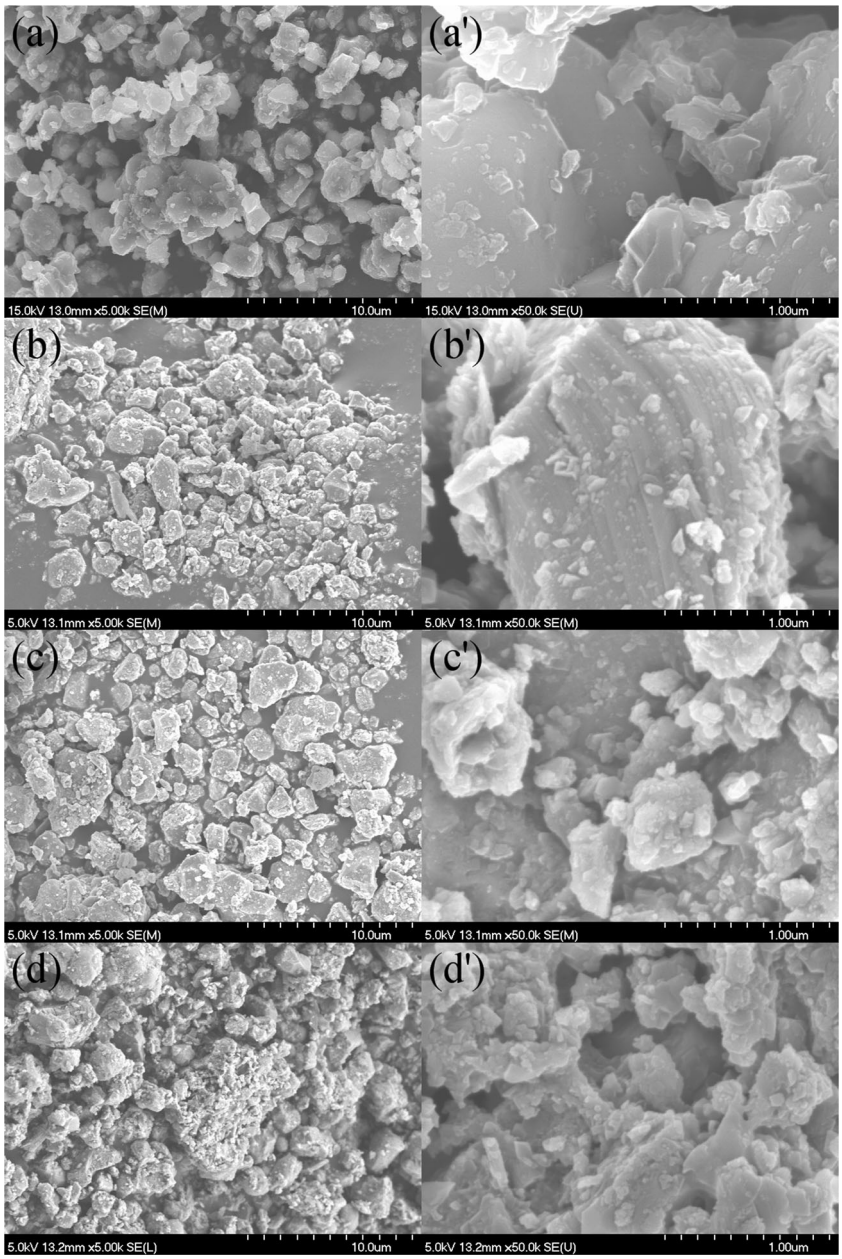

Fig. 2 SEM images of LNCMO (**a**, **a'**), 1 wt% LZO-LNCMO (**b**, **b'**), 3 wt% LZO-LNCMO (**c**, **c'**), 5 wt% LZO- LNCMO (**d**, **d'**) with two magnifications

XRD data based on Rietveld refinement. The lattice parameters of the pristine power were a=2.871466 Å and c= 14.220705 Å. The results match well with the values observed by Ohzuku and Makimure (a=2.867 Å and c=14.246 Å) [9]. These values of the coated samples are close to the pristine material with 2.871466 and 14.220705 Å, indicating that the Li_2ZrO_3 coating does not influence the $LiNi_{0.6}Co_{0.2}Mn_{0.2}O_2$ host structure. As shown in Table 1, the value of c/a is almost the same among these samples, which further indicate that the lattice structure of $LiNi_{0.6}Co_{0.2}Mn_{0.2}O_2$ still remains before and after Li_2ZrO_3 coating.

The integrated intensity ratio of $I_{(003)}/I_{(104)}$ has been considered as a measurement of cation disorder and had a direct impact on the electrochemical properties of the system [28]. Generally, when I(003)/I(104)>1.2, the positive-electrode material has a good layered structure due to the small cation mixing. The oxygen sublattice in the α-$NaFeO_2$ type structure is distorted from the fcc array in the direction of hexagonal c-axis. This distortion gives rise to a splitting of the lines assigned to the Miller indices (006)/(102) and (108)/(110) in the XRD patterns, which is the characteristic of the layered structure. The hexagonal lattice parameters, a and c, as well as the c/a and $I_{(003)}/I_{(104)}$ are presented in Table 1. These parameters were obtained by Rietveld refinement with the GSAS software. As shown in Table 1, lattice parameters of all samples vary obviously with Li_2ZrO_3 content. Lattice parameters a and c increase with increasing of Li_2ZrO_3 content, which should be some Zr^{4+} has diffused into the parent oxide after

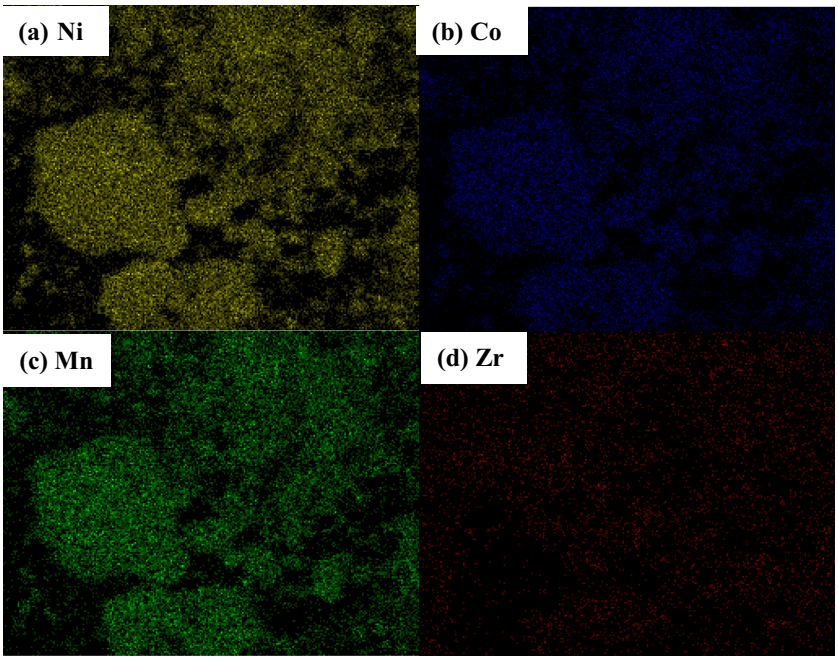

Fig. 3 The elemental mappings of 1 wt% LZO-LNCMO

the high-temperature treatment [18]. Besides, 1 % Li_2ZrO_3 coating material with the largest value of ratio $I_{(003)}/I_{(104)}$ is expected to show the best electrochemical performance. In addition, all the XRD patterns show a clear splitting between the (006)/(102) and (108)/(110) peaks which confirms that these samples have good layered characteristics.

The surface morphology of the bare and Li_2ZrO_3-coated powers is shown in Fig. 2. It can be seen that all the samples have good bulk shape with particle size range from 5 to 15 μm. There are no significant differences between those images. However, the surface morphologies of the coated sample become rough. As seen in Fig. 2b, b', the Li_2ZrO_3

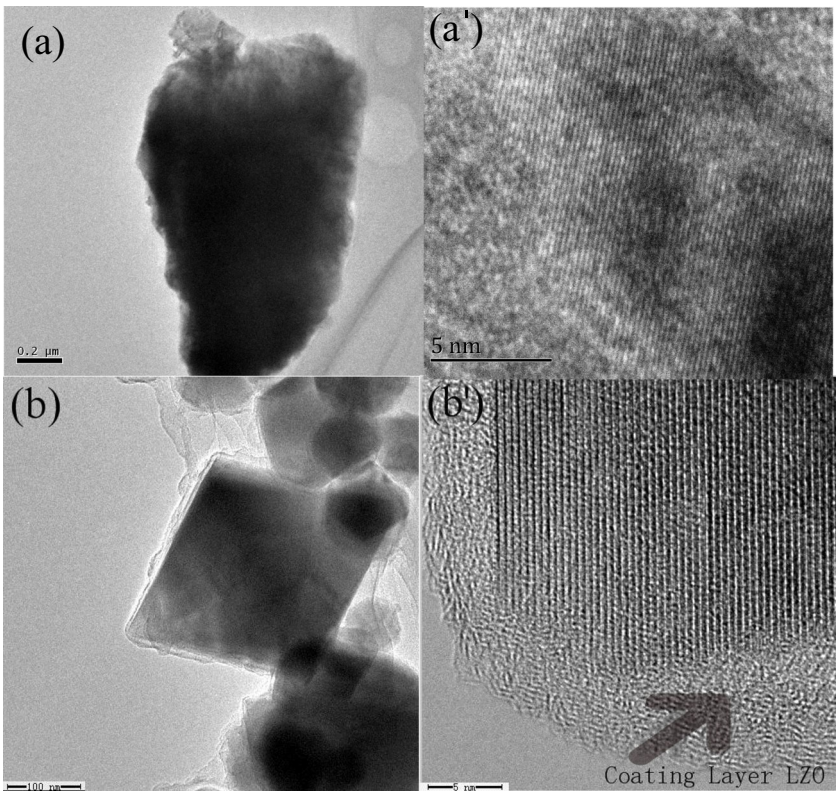

Fig. 4 TEM images of the LNCMO (**a**, **a'**) and the 1 wt% LZO-LNCMO (**b**, **b'**)

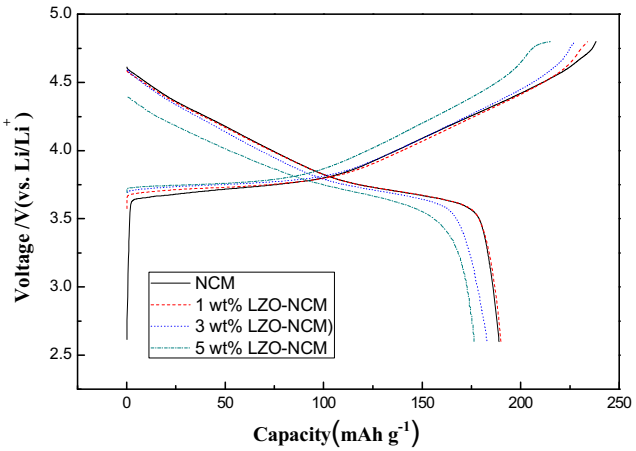

Fig. 5 The initial charge–discharge curves of the bare and Li_2ZrO_3-coated $LiNi_{0.6}Co_{0.2}Mn_{0.2}O_2$

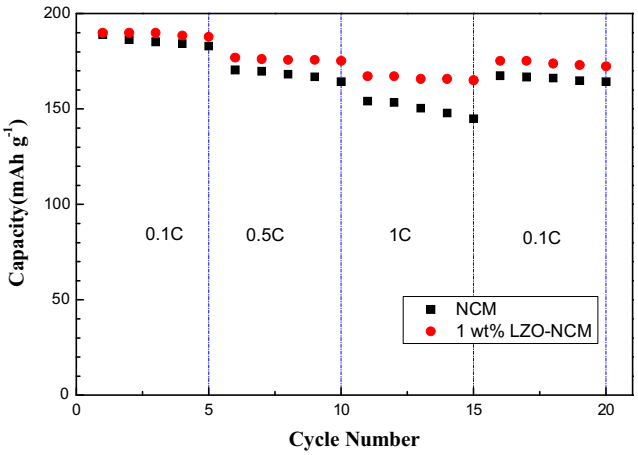

Fig. 7 Rate performance of the bare and 1 wt% Li_2ZrO_3-coated $LiNi_{0.6}Co_{0.2}Mn_{0.2}O_2$

particle was distributed uniformly on the surface of the LNCM particle even though it is hard to distinguish the thickness of the coating layer from the SEM picture. The thin layer on the surface was expected to result in better cycling performance and enhanced thermal stability. The composition and distribution of elements on the surface of 1 wt.% Li_2ZrO_3-modified $LiNi_{0.6}Co_{0.2}Mn_{0.2}O_2$ were examined by EDS, as shown in Fig. 3. EDS can corroborate that 1 wt.% LZO-LNCM sample includes the elements of Ni, Co, Mn, and Zr. The EDS dot mappings (Fig. 3a–d) show that the elements of Ni, Co, Mn, and Zr in 1 wt.% LZO-LNCM sample are homogeneously distributed.

In order to further clarify the nanoscale microstructure of the sample, TEM investigation was conducted. As shown in Fig. 4, the pristine sample exhibited a smooth surface. On the other hand, the coated samples have a rough and porous coating layer with a thickness of 5 nm. The homogeneous Li_2ZrO_3 coating layer not only improve the diffusion ability between the bulk of $LiNi_{0.6}Co_{0.2}Mn_{0.2}O_2$ and the electrolyte but also protect active material from the side reactions with the sulfide electrolyte [18, 29].

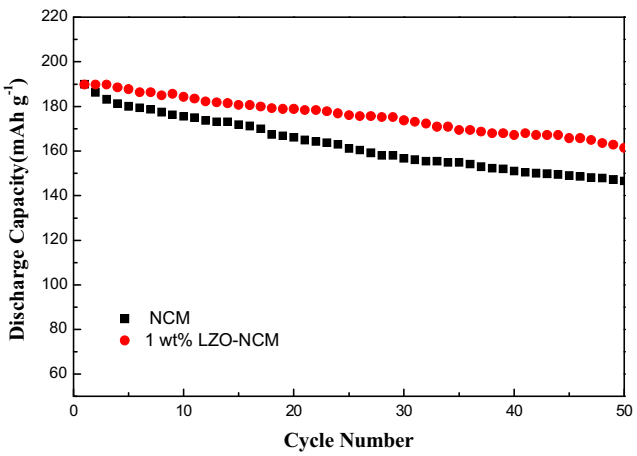

Fig. 6 The cycle performance curves of the bare and 1 wt% Li_2ZrO_3-coated $LiNi_{0.6}Co_{0.2}Mn_{0.2}O_2$

In order to study the electrochemical performance of the Li_2ZrO_3-coated samples with different amounts of Li_2ZrO_3, coin cells were operated at 0.1 C (1 C=274 mAh g^{-1}) over the voltage range of 2.6 to 4.8 V at room temperature. The initial charge/discharge performance of the pristine and the coated samples are shown in Fig. 5. These results indicate that the charging and discharging curves of all cells are quite smooth. Comparing with the curves of the pristine and Li_2ZrO_3-coated samples, the charge curve of the later is higher than the former, which indicates that a resistive coating layer exists in the surface of the Li_2ZrO_3-coated samples. The initial charge and discharge capacities of the pristine $LiNi_{0.6}Co_{0.2}Mn_{0.2}O_2$ are 233 and 189 mAh g^{-1}, respectively. However, the charge and discharge capacity first increases then decreases with the increasing of Li_2ZrO_3 content. The charge and discharge capacity are 234 mAh g^{-1} and 190 mAh g^{-1}, 227 mAh g^{-1} and 183 mAh g^{-1}, 215 mAh g^{-1} and 177 mAh g^{-1} for 1, 3, 5 wt% Li_2ZrO_3-coated samples, respectively. Thus, 1.0 wt.% Li_2ZrO_3-coated samples have the highest electrochemical performancs, which is well consistent with the XRD tests. A small amount of Li_2ZrO_3 that exists on the surface can suppress the oxygen activity and decrease polarization by introducing strong metal-oxygen bonds which act as the conductive for Li^+ [30]. However, Li_2ZrO_3 is an electrochemical inactive material; so, too much Li_2ZrO_3 on the surface of the material will lead to capacity loss due to a decrease in active material [29]. Due to a lower capacity of the 3 and 5 wt% Li_2ZrO_3-coated sample, further studies on cycling performance and rate capability are carried out only for bare and 1 wt% Li_2ZrO_3-coated sample.

The cycling stability for the two materials using a half cell at 0.1 C was studied, and the results are shown in Fig. 6. It can

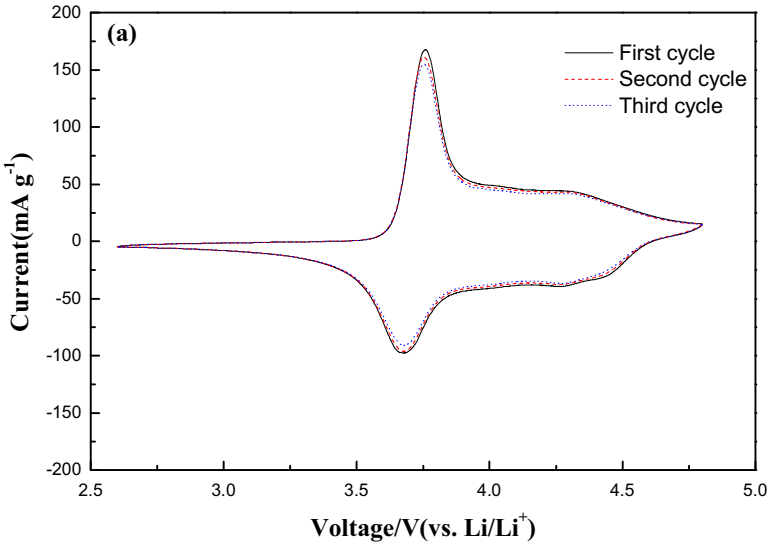

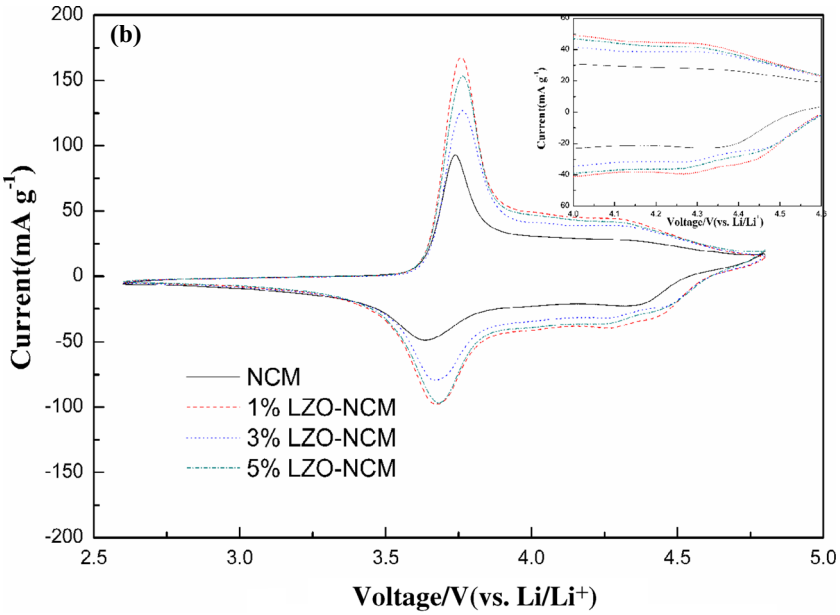

Fig. 8 Cyclic voltammetric curves of the first three cycles of 1 wt% LZO-NCM (**a**) and the second cycle of the bare and Li_2ZrO_3-coated $LiNi_{0.6}Co_{0.2}Mn_{0.2}O_2$ (**b**)

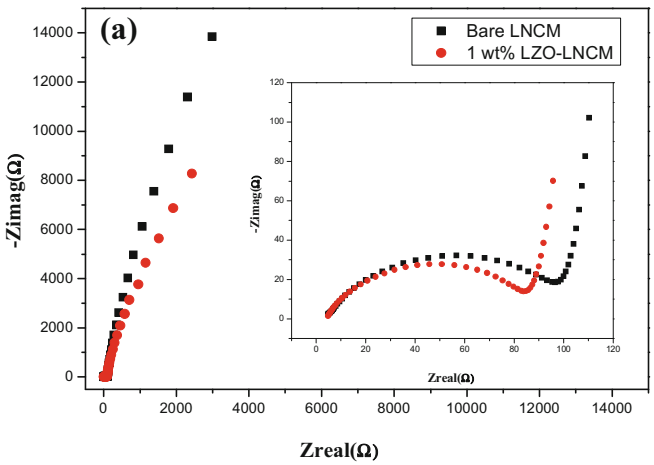

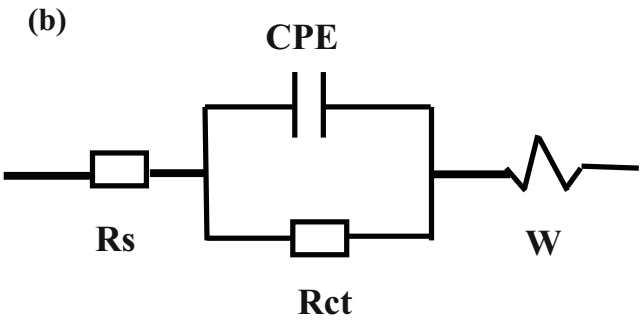

Fig. 9 Nyquist plots (**a**) and the equivalent circuit (**b**) used to interpret the impedance results of bare and 1 wt% Li_2ZrO_3-coated $LiNi_{0.6}Co_{0.2}Mn_{0.2}O_2$

Table 2 Impedance parameters derived from the equivalent circuit for $LiNi_{0.6}Co_{0.2}Mn_{0.2}O_2$ (LNCMO) and 1 wt.% Li_2ZrO_3-coated $LiNi_{0.6}Co_{0.2}Mn_{0.2}O_2$

Samples	R_s (Ω cm^{-2})	CPE-T (10^{-5} S cm^{-2})	CPE-P (S cm^{-2})	R_{ct} (Ω cm^{-2})	Chi-squared
LNCMO	3.838	4.2005	0.69286	105.6	0.0004368
1 wt% LZO-LNCMO	4.011	3.3685	0.73007	86.59	0.0003583

be observed that the capacity of $LiNi_{0.6}Co_{0.2}Mn_{0.2}O_2$ drop to 147 mAh g^{-1} after 50 cycles at 0.1 C, with a capacity retention of 78 %. However, the Li_2ZrO_3-coated sample demonstrated remarkably improved cycling stability with a capacity retention of 85 % after 50 cycles. The capacity loss for the bare sample should be ascribed to several factors, such as cation mixing, side reaction between electrode and electrolyte, and transition metal ion dissolution. The Li_2ZrO_3 coating layer can prevent the direct contact of the electrode materials from electrolyte, and thus suppress the undesirable side reaction between them and the dissolution of the transition metal elements [31, 32].

The rate capability behaviors of the pristine and the 1 wt% Li_2ZrO_3-coated $LiNi_{0.6}Co_{0.2}Mn_{0.2}O_2$ were investigated upon progressive cycling as a function of different current densities. Each cell was charged at the same rate of 0.1 C between 2.6 and 4.8 V under room temperature, and then discharged at different rate of 0.1, 0.5, 1, and 0.1 C, respectively. As can be seen in Fig. 7, the discharge capacities of both samples are nearly the same at 0.1 C rate. As the C rate increased, the discharge capacities of the pristine and the coated samples decrease, this was due to the increased polarization at high charge–discharge rates. However, the capacity loss of bare $LiNi_{0.6}Co_{0.2}Mn_{0.2}O_2$ is slightly larger than that of the Li_2ZrO_3-coated $LiNi_{0.6}Co_{0.2}Mn_{0.2}O_2$ at higher rates. Thus, minor Li_2ZrO_3 coating can improve the rate performances and cycle stability, which is in accordance with the above results.

Cyclic voltammetry (CV) analysis is taken to further understand the effect of Li_2ZrO_3 coating in improving the electrochemical property of $LiNi_{0.6}Co_{0.2}Mn_{0.2}O_2$. The cells were tested at a scan rate of 0.1 mV s^{-1} after being discharged to 2.6 V for three cycles. Figure 8 shows the CV curves for the first three cycles of the 1 wt% Li_2ZrO_3-coated $LiNi_{0.6}Co_{0.2}Mn_{0.2}O_2$ sample. A pair of sharp redox peaks located at 3.76 V/3.62 V was observed from the initial CV curve. During the subsequent cycles, the oxidation peaks shifted to 3.7 V while the reduction peaks remained unchanged. The stable small gap of the redox reaction peaks from the second cycle indicates the cycle stability of the coated sample. Figure 8b shows the second cycle of CV curves for different amounts of Li_2ZrO_3-coated cathode materials. Based on the CV results, all the samples have two couples of redox peaks (one obvious redox peaks and one less discernable) in the voltage range between 2.6 and 4.8 V. The Ni^{2+}/Ni^{4+} account for the obvious oxidation peak around 3.7 V and the reduction peak around 3.6 V, the other less discernable oxidation peaks around 4.35 V indicated the multiphase transitions of hexagonal (H2) to another hexagonal (H3) [33, 34]. The corresponding reduction peaks were present at 4.28 V. It has been reported that the rapid volume contraction during the structural transformation from H2 to H3 mostly affects the capacity fading of the $Li[Ni_xCo_yMn_z]O_2$ [35, 36].

The thin layer of Li_2ZrO_3 coating suppresses the multiphase transitions and improve the cycle performances, which is consistent with previous report [37].

Furthermore, electrochemical impedance spectroscopy (EIS) is used to analyze the electrochemical properties of the pristine and 1 wt% Li_2ZrO_3-coated sample after 10th cycles at 0.1 C rate between 2.6 and 4.8 V vs Li/Li^+. All the cells were measured at fully discharge state at room temperature. As shown in Fig. 9a, the Nyquist plots of the cells consist a semicircles in appearance of a half ellipse (in the high and intermediate frequency ranges) and a straight line with changing slope to the real axes (in the lower frequency range). The study of the EIS results has been performed by using the approach outlined in Ref. [38, 39] and an equivalent circuit model shown in Fig. 9b. The fitting results derived from the equivalent circuit are presented in Table 2. Generally, an intercept at the Zreal axis at a high frequency corresponds to the ohmic resistance (Rs), which represents the total resistance of the electrolyte, separator, and electrical contacts. The semicircle in the high and intermediate frequency ranges indicates the charge transfer resistance (Rct). The inclined line in the lower

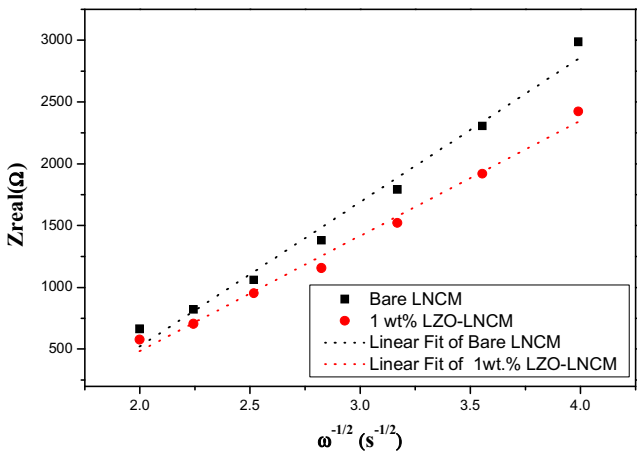

Fig. 10 Zre as a function of square root of frequency for bare and 1 wt% Li_2ZrO_3-coated $LiNi_{0.6}Co_{0.2}Mn_{0.2}O_2$ at low frequency

frequency range represents the Warburg impedance and corresponds to the lithium diffusion kinetics toward the electrodes. As shown in Table 2, the electrolyte resistance remained almost constant, which was expected since the variation of an electrolyte concentration was not so large as to affect the electrolyte conductivity. The charge transfer resistance (Rct) of 1 wt.% Li_2ZrO_3-coated $LiNi_{0.6}Co_{0.2}Mn_{0.2}O_2$ is smaller than the bare $LiNi_{0.6}Co_{0.2}Mn_{0.2}O_2$, indicating that the 1 wt.% Li_2ZrO_3 coating improves the kinetic behavior of intercalation and deintercalation of Li^+ (Fig. 10).

In order to clarify the effect of Li_2ZrO_3 coating on the Li^+ conductivity of $LiNi_{0.6}Co_{0.2}Mn_{0.2}O_2$ material, lithium-ion diffusion coefficient D_{Li+} could be obtained from the slope in the low frequency according to the following equation [36]:

$$DLi^+ = \frac{R^2T^2}{2A^2n^4F^4C^2\sigma^2} \quad (1)$$

Here, R is the gas constant (R=8.314 J mol^{-1} k^{-1}), T is the absolute temperature (T=298.15 K), A is the cathode surface area (A=0.785 cm^2), n is the number of electrons per molecule during oxidization (n=1), F is the Faraday constant (F= 96485.34 C mol^{-1}), C is the lithium-ion concentration, and σ is the Warburg factor. The Warburg factor can be calculated according to the following equation:

$$Z_{re} = R_s + R_{ct} + \sigma\omega^{-1/2} \quad (2)$$

Here, ω is the low frequency. Figure 9 illustrates the relationship between Zre and square root of frequence ($\omega^{-1/2}$) in the low frequency region. According to Eqs. (1) and (2), we can calculate the value of D_{Li+} and σ are 1.75768×10^{-11} cm^2 s^{-1}, 1.1685×10^3 Ω $s^{-1/2}$ and 2.75866×10^{-11} cm^2 s^{-1}, 0.9327×10^3 Ω $s^{-1/2}$ for the bare and 1.0 wt.% Li_2ZrO_3 coating samples, respectively. Thus, minor Li_2ZrO_3 coating not only suppress the active materials with electrolyte, but also increase the diffusion of Li^+ and improve the high-rate capacity and cycleability.

Conclusions

In this report, a Li_2ZrO_3 coating layer was prepared on the surface of $LiNi_{0.6}Co_{0.2}Mn_{0.2}O_2$ material via a wet chemical method. The effect of Li_2ZrO_3 modification on the performance of $LiNi_{0.6}Co_{0.2}Mn_{0.2}O_2$ was investigated. After Li_2ZrO_3 coating, the LNMO remains the crystal structure and lattice parameters. The surface coating layer of Li_2ZrO_3 can improve the cycle performance by suppressing the side reaction between the electrode and the electrolyte. The charge–discharge test indicated that 1 wt% Li_2ZrO_3-modified material shows a better cycle performance and rate capability. The Li_2ZrO_3-coated electrode delivers the capacity of 189 mAh g^{-1} and remains 161 mAh g^{-1} after 50 cycles with a capacity retention about 85 % in the voltage range between 2.6 to 4.8 V. EIS results show that the charge transfer resistance was suppressed, and the Li^+ diffusion was improved significantly by Li_2ZrO_3 modification. As a host structure material for Li^+, Li_2ZrO_3 is a more competitive candidate for electrode material modification, and it has a great potential application in other cathode materials.

Acknowledgments This work is supported by the project of Innovative group for high-performance lithium-ion power batteries R&D and industrialization of Guangdong Province (Grant No. 2013N079), Shenzhen Peacock Plan Program (KQCX20140521144358003), Fundamental research plan of Shenzhen (JCYJ20140417172417144) and State Key Laboratory of Chemical Engineering (No. SKL-ChE-14B04).

References

1. Park BG, Kim SH, Kim ID, Park YJ (2010) J Mater Sci 45:3947
2. Goodenough JB (2007) J Power Sources 174:996
3. Woo SW, Myung ST, Bang H, Kim DW, Sun YK (2009) Electrochim Acta 54:3851
4. Konarova M, Taniguchi I (2009) J Power Sources 194:1029
5. Kim TH, Park JS, Chang SK, Choi S, Ryu JH, Song HK (2012) Adv Energy Mater 2:860
6. Lee DJ, Scrosati B, Sun YK (2011) J Power Sources 196:7742
7. Jouanneau S, MacNeil DD, Lu Z, Beattie SD, Murphy G, Dahn JR (2003) J Electrochem Soc 150:A1299
8. Santhanam R, Jones P, Sumana A, Rambabu B (2010) J Power Sources 195:7391
9. Ohzuku T, Makimura Y (2001) Chem Lett 30:642
10. Shaju KM, Bruce PG (2007) J Power Sources 174:1201
11. Choi J, Manthiram A (2005) J Electrochem Soc 152:A1714
12. Kim HS, Kong M, Kim K, Kim IJ, Gu HB (2007) J Power Sources 171:917
13. Na SH, Kim HS, Moon SI (2005) Solid State Ion 176:313
14. Myung ST, Izumi K, Komaba S, Sun YK, Yashiro H, Kumagai N (2005) Chem Mater 17:3695
15. Liu MH, Hang HT, Lin CM, Chen JM, Liao SH (2014) Electrochim Acta 120:133
16. Chen DR, Li BZ, Liao HL, Lan HW, Lin HB, Xing LD, Wang YT, Li WS (2014) J Solid State Electrochem 18:2027
17. Chang W, Choi JW, Im JC, Lee JK (2010) J Power Sources 195: 320–326
18. Huang YY, Chen JT, Ni JF, Zhou HH, Zhang XX (2009) J Power Sources 188:538–545
19. Feng LJ, Wang SP, Han L, Qin XY, Wei HY, Yang YZ (2012) Mater Lett 78:116–119
20. Lee JW, Park SM, Kim HJ (2009) J Power Sources 188:583
21. Zhang J, Xiang YJ, Yu Y, Xie S, Jiang GS, Chen CH (2004) J Power Sources 132:187
22. Cao H, Xia B, Zhang Y, Xu N (2005) Solid State Ion 176:911
23. Park SC, Han YS, Kang YS, Lee PS, Ahn S, Lee HM, Lee JY (2001) J Electrochem Soc 148:A680
24. Cong LN, Gao XG, Ma SC, Guo X, Zeng YP, Tai LH, Wang RS, Xie HM, Sun LQ (2014) Electrochi Acta 115:399
25. Wang JH, Wang Y, Guo YZ, Ren ZY, Liu CW (2013) J Mater Chem A 1:4879
26. Kim HS, Kim Y, Kim SI, Martin SW (2006) J Power Sources 161: 623
27. Miao XW, Ni H, Zhang H, Wang CG, Fang JH, Fang G (2014) J Power Sources 264:147

28. Ohzuku T, Ueda A, Nagayama M (1993) J Electrochem Soc 140: 1862
29. Thackeray MM, Johnson CS, Kim JS, Lauzze KC, Vaughey JT, Dietz N, Abraham D, Hackney SA, Zeltner W, Anderson MA (2003) Electrochem Commun 5:752
30. Song HK, Lee KT, Kim MG, Nazar LF, Cho J (2010) Adv Funct Mater 20:3818
31. Shaju KM, Rao GVS, Chowdari BVR (2004) J Electrochem Soc 151:1324
32. Lee HJ, Park KS, Park YJ (2010) J Power Sources 195:6122
33. Song MY, Lee DS, Park HR (2012) Mater Res Bull 47:1021
34. Bak YR, Chung Y, Ju JH, Hwang MJ, Lee Y, Ryu KS (2011) J New Mater ElectrochemSyst 14:203
35. Woo SU, Yoon CS, Amine K, Belharouak I, Sun YK (2007) J Electrochem Soc 154:A1005
36. Noh HJ, Youn S, Yoon CS, Sun YK (2013) J Power Sources 233:121
37. Cho J, Kim TJ, Kim YJ, Park B (2001) Electrochem Solid State Lett 4:A159
38. Yang M, Du CQ, Tang ZY, Wu JW, Zhang XH (2014) Ionics 20:1039
39. Jang IC, Son CG, Yang SMG, Lee JW, Cho AR, Aravindan V, Park GJ, Kang KS, Kim WS, Cho WI, Lee YS (2011) J Mater Chem 21: 6510